Molecular Therapy
Original Article

# Fetal Gene Therapy Using a Single Injection of Recombinant AAV9 Rescued SMA Phenotype in Mice

Afrooz Rashnonejad,[1,7] Gholamhossein Amini Chermahini,[2] Cumhur Gündüz,[3] Hüseyin Onay,[4] Ayça Aykut,[4] Burak Durmaz,[4] Meral Baka,[5] Qin Su,[6] Guangping Gao,[6] and Ferda Özkınay[4]

[1]Department of Biotechnology, Ege University, Izmir 35100, Turkey; [2]Faculty of Medicine, Ege University, Izmir 35100, Turkey; [3]Department of Medical Biology, Faculty of Medicine, Ege University, Izmir 35100, Turkey; [4]Department of Medical Genetics, Faculty of Medicine, Ege University, Izmir 35100, Turkey; [5]Department of Histology and Embryology, Faculty of Medicine, Ege University, Izmir 35100, Turkey; [6]The Horae Gene Therapy Center, University of Massachusetts Medical School, Worcester, MA 01605, USA

**Symptoms of spinal muscular atrophy (SMA) disease typically begin in the late prenatal or the early postnatal period of life. The intrauterine (IU) correction of gene expression, fetal gene therapy, could offer effective gene therapy approach for early onset diseases. Hence, the overall goal of this study was to investigate the efficacy of human survival motor neuron (*hSMN*) gene expression after IU delivery in SMA mouse embryos. First, we found that IU-intracerebroventricular (i.c.v.) injection of adeno-associated virus serotype-9 (AAV9)-EGFP led to extensive expression of EGFP protein in different parts of the CNS with a great number of transduced neural stem cells. Then, to implement the fetal gene therapy, mouse fetuses received a single i.c.v. injection of a single-stranded (ss) or self-complementary (sc) AAV9-SMN vector that led to a lifespan of 93 (median of 63) or 171 (median 105) days for SMA mice. The muscle pathology and number of the motor neurons also improved in both study groups, with slightly better results coming from scAAV treatment. Consequently, fetal gene therapy may provide an alternative therapeutic approach for treating inherited diseases such as SMA that lead to prenatal death or lifelong irreversible damage.**

## INTRODUCTION

Spinal muscular atrophy (SMA) is the second most common cause of newborn mortality (a prevalance of 1–2/100,000 individuals), after cystic fibrosis (CF) (prevalence of 0.737/10,000 individuals).[1,2] Homozygous deletions in the survival motor neuron (*SMN*) gene cause a reduced level of the SMN protein, leading to the disease.[3] Five different types of autosomal recessive inherited SMA types (types 0, I, II, III, and IV) have been classified, according to the age at onset, clinical presentation of the disease, and the severity. Symptoms of the most severe forms of SMA (types 0 and I) appear from the late prenatal to the early postnatal period and include: decreased movement at prenatal stage, fetal akinesia sequence, congenital contractures, and postnatal respiratory insufficiency.[4–6] Fetal gene therapy presents as a promising approach to prevent irreversible tissue damage caused by early onset genetic disorders that require early childhood treatments, such as SMA, Duchenne muscular dystrophy (DMD), CF, and lysosomal storage diseases. Restoring the defective gene function at an older age is only capable of halting progression of the disease but is not generally able to reverse the pathological alterations and, therefore, cannot provide complete cures for these diseases.[7] Fetal gene therapy offers the advantage of delivering therapeutic transgenes prior to disease onset and complete development of immune system, called "preimmunity." Fetal gene therapy during this phase, utilizing both central and peripheral mechanisms of tolerance induction, leads to the development of immune tolerance.[8] Another advantage of fetal gene therapy is that delivering of transgene into the stem cells provides longer gene expression and reduces the necessity for further re-administration.[9] In the case of CNS diseases, transducing neural stem cells after birth is extremely challenging. Thus, intrauterine (IU) correction of neuronal cells seems to present as a logical treatment for prenatally fatal neurodegenerative disorders or those that show severe postnatal progression due to difficulties associated with accessing the CNS during the postnatal period.

The ability of adeno-associated virus (AAV) to deliver SMA therapeutic vectors has previously been demonstrated to transduce motor neurons and alleviate disease symptoms in both preclinical[10–12] and clinical studies for SMA gene therapy.[13,14] These studies finally led to the first FDA-approved AAV-based gene therapy treatment for this disease.[15] With these promising advancements in the field of gene therapy, we thought that the next step could be testing gene therapy treatments in an earlier developmental stage, specifically, for severe types of SMA (type 0/1) in which symptoms start even

Received 1 February 2019; accepted 12 August 2019;
https://doi.org/10.1016/j.ymthe.2019.08.017.

[7]Present address: Center for Gene Therapy, Abigail Wexner Research Institute at Nationwide Children's Hospital, 700 Children's Drive, Columbus, OH 43215, USA.

**Correspondence:** Afrooz Rashnonejad, Center for Gene Therapy, Abigail Wexner Research Institute at Nationwide Children's Hospital, 700 Children's Drive, Columbus, OH 43215, USA.
**E-mail:** afrooz.rashnonejad@nationwidechildrens.org

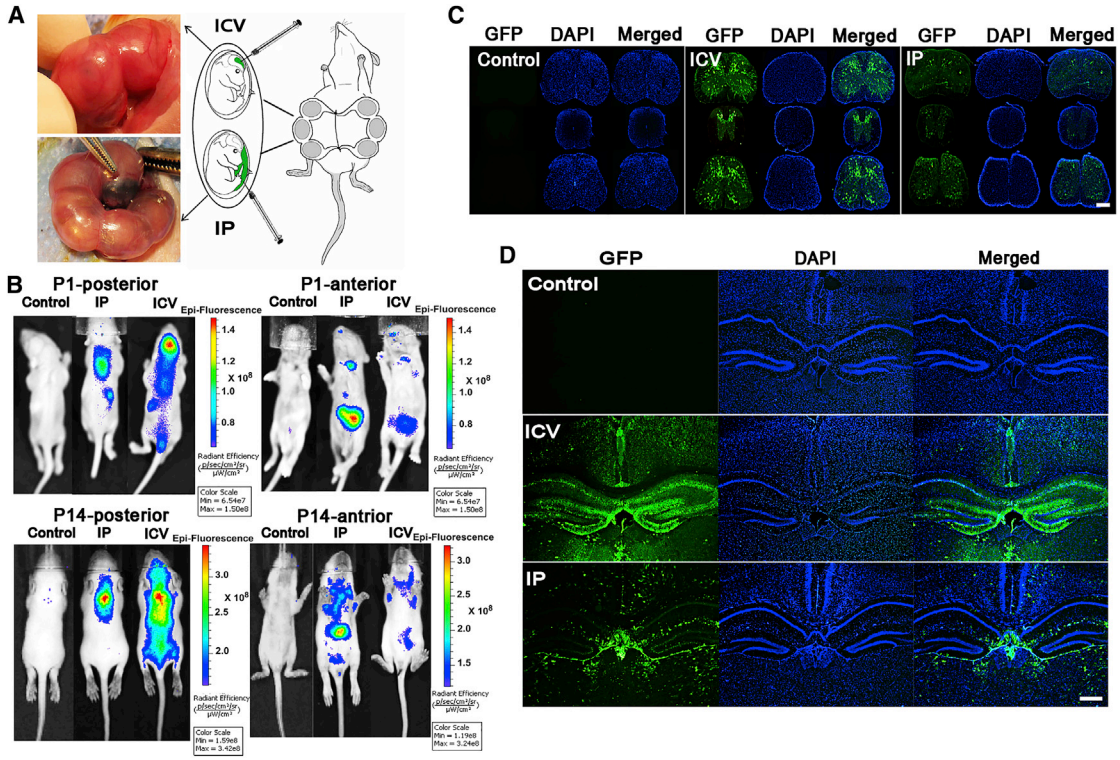


**Figure 1. Biodistribution of rAAV9-EGFP in CNS**

(A) IP and i.c.v. injections into E14–E15 mouse embryos. (B) IVIS imaging results at P1 and P14. The higher level of EGFP fluorescent signal was seen in the brain of pups that were administered i.c.v. injections from posterior view. In the anterior view of P1 and P14 pups; the liver of pups that were administered IP injections showed high GFP expression among internal organs. The level of EGFP expression was detected in both pups that received i.c.v. injections and those that received IP injections, specifically in intrascapular (posterior view) and inguinal (anterior view) regions known as BAT places. (C and D) Representative images of (C) cervical, thoracic, and lumbar spinal cord and (D) the brain's coronal sections show a higher EGFP expression in the CNS regions of the mice receiving i.c.v. injections at P30. 4× objective. Scale bar, 500 μm.

before birth. However, very little information is available concerning the distribution and transduction efficiency of self-complementary AAV serotype-9 (scAAV9) after IU administration. Taking this into consideration, we first investigated the neuronal transduction patterns of the brain and spinal cord following the IU-intracerebroventricular (i.c.v.) and intraplacental (IP) injection of scAAV9-EGFP to mouse fetuses at embryonic day 15 (E15). After determining the most efficient method for transgene delivery into the neurons and motor neurons, we replaced GFP vectors with our therapeutic AAV9-SMN for delivery to SMA embryos at E15. The results of this study demonstrate the utility of fetal gene therapy for SMA and pave the way for future studies to find an early treatment for this disease before appearance of irreversible symptoms.

## RESULTS

### *In Vivo* Imaging of GFP Expression in Prenatally Injected Mice

The IU injection method and the number of live-born fetuses in the pilot study are shown in Figure 1A and Table S1, respectively. The overall goal of the pilot study was to investigate the CNS transduction efficiency via two different injection methods: IU-i.c.v. and IU-IP injection. The AAV9 vector transduction profile was monitored *in vivo* in the neonates receiving IU injections at post-natal day (P)1 and P14 using the *in vivo* imaging system (IVIS). The levels of fluorescence related to EGFP at P1 and P14 are shown in Figure 1B. In pups that were administered i.c.v. injections, the maximum GFP expression was detected in the brain at P1; however, high levels were also shown in the spinal cord at P14. The EGFP-related fluorescent signal showed an increase over time in the interscapular region of almost all pups in both groups (Figure 1B). From the anterior view (Figure 1B), the fluorescent signal showed a higher intensity in the liver and inguinal regions of mice receiving IP injections compared to the same regions in mice receiving i.c.v. injections. To demonstrate EGFP expression in different parts of the brain and spinal cord, immunofluorescent analysis was performed.

### AAV9-Mediated GFP-Positive Neurons in Brain and Spinal Cord

One month postpartum (P30), fluorescent microscopy analysis of mouse spinal cord and brain sections revealed extensive GFP expression in both the i.c.v. and IP injection groups (Figures 1C and 1D). The IP group showed higher homogeneity in EGFP-transduced cells in the brain, while the i.c.v. injection group

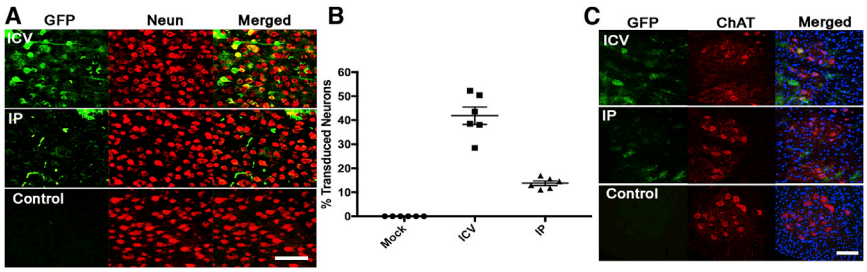


**Figure 2. Transduction of Neurons in Prenatally Injected Pups at P30**

(A) EGFP-positive cells in the cortex of mice that were administered i.c.v. and IP injections. (B) The percentages of AAV9-transduced neurons, co-expressed with EGFP and NeuN, in the cortex (n = 6). (C) AAV9-EGFP transduced motor neurons in spinal cord more efficiently via i.c.v. injection. 20× objective. All scale bars, 100 μm. $p < 0.0001$, by Student's unpaired two-tailed t test.

showed higher EGFP expression in the dentate gyrus regions (Figure 1D). Robust transduction in the cortex, dentate gyrus (DG), and choroid plexus (CP) regions was observed in the i.c.v.-injection-group mouse brain (Figure 1D). Strong transduction of the CP regions in both groups demonstrates recombinant AAV9 (rAAV9) tropism for cells located in this region of brain (Figure S1). To compare transduction profiles of the two different vector administration routes at the cellular level, prefixed micrographs were stained with various anti-neuronal antibodies and analyzed with fluorescent microscopy. The number of GFP+ cells co-localized with NeuN+ cells (Figure 2A, yellow) was found to be highest in the cortex and hippocampus (DG) (Figure S2) regions of brain from mice that received an i.c.v. injection. In contrast, the highest expressing brain regions from the mice administered an IP injection were the thalamus and hypothalamus (Figure S3). As shown in Figures 2A and 2B, the number of transduced neurons by AAV9-EGFP vector in the cortex of mice that received i.c.v. injections is higher (41% ± 8.8%) than that in subjects that received IP injections (13.8% ± 2.26%). In addition, the positive neurons in the cortex tissue samples of the cases with IP injections exhibited a very weak GFP signal. While the IP administration route led to a higher number of GFP+ cells with glial or astrocyte morphology, the i.c.v.-injection-mediated GFP expression was mostly restricted to neurons, making it a superior method for SMA treatment.

Cells in both the dorsal and anterior horns of all spinal cord samples were transfected; however, spinal cord samples from subjects that received IP injections showed low GFP expression patterns similar to those of the brain samples (Figure 1C). In mice that received i.c.v. injections, the majority of transduced neurons were found to be located in the anterior horns of the spinal cords, while those that received IP injections had very few GFP+ neurons (Figure S4). To investigate motor neuron transduction by AAV9-EGFP in the spinal cord, some sections were stained with anti-choline acetyltransferase (ChAT) antibody. As shown in Figure 2C, the motor neurons were successfully transduced in both groups, with a higher number in mice that received i.c.v. injections. To compare the transduction efficiency of astrocytes in spinal cord samples of the two study groups, some sections were stained with anti-glial fibrillary acidic protein (GFAP) antibody. While the transduced astrocytes can be seen in the spinal cord micrographs of both the i.c.v. samples and the IP samples, the numbers are slightly higher in the IP samples (Figure S5). Colocalization of GFP protein and Nestin was detected in certain cells from both mice receiving i.c.v. injections and mice receiving IP injections prenatally (Figure S6).

### Quantification by Western Blot of EGFP Expression in Mice Given IU Injections

Western blot analysis was performed to reveal EGFP protein quantities in the brain, spinal cord, and other internal organs of injected mice (Figure 3). The highest EGFP protein levels were found to be in the hippocampus (23.2-fold) mice that received i.c.v. injections (Figures 3A and 3C). As shown in Figures 3B and 3D, among internal organs, the liver and brown adipose tissue (BAT) of mice that received IP injections exhibited elevated levels of EGFP 19.76-fold and 18.3-fold, respectively. In mice that received i.c.v. injections, different parts of the brain showed significantly higher EGFP expression when compared to those observed in mice receiving IP injections. However, as seen in the immunofluorescence (IF) analysis, the thalamus region of the IP-injection mice showed higher EGFP protein levels (Figures 3A and 3C) when compared to the same region in the i.c.v.-injected subjects. The increased levels of EGFP protein in the spinal cord of the i.c.v.-injected mice, when compared to those in the IP-injection mice, (17.7-fold and 4.5-fold, respectively) revealed that the AAV9 had been well distributed via cerebrospinal fluid (CSF). Western blot results confirmed a transgene expression in the brain and spinal cord by AAV9 vectors in 1-month-old mice that received i.c.v. injections. Following IP injections, western blot results showed higher distribution rates of AAV9 vector into internal organs—specifically, liver and BAT—when compared to i.c.v. injection.

### Increased Survival and Rescued SMA Phenotype in Prenatally Treated Mice

The overall goal of this study was to investigate the efficacy of fetal gene therapy for SMA disease in the SMNΔ7 mouse model. Due to a difference in the transgene-carrying capacity of single-stranded (ss)- and scAAV vectors, we designed two vectors with slight differences in their transgene cassettes. While the ssAAV9-SMN vector carries complete SMN cDNA with its specific UTRs, scAAV9-SMN contains SMN cDNA without its UTRs.[16] Both transgenes contain a CMV enhancer/chicken beta-actin (CB) promoter, poly(A) signal, and one small intron.[16] Then, we investigated the efficacy of ss- and scAAV9-SMN for fetal gene therapy in SMA mice. The i.c.v.-injection route was chosen as our vector administration route for fetal gene therapy studies of SMA based on preliminary data from our pilot studies.

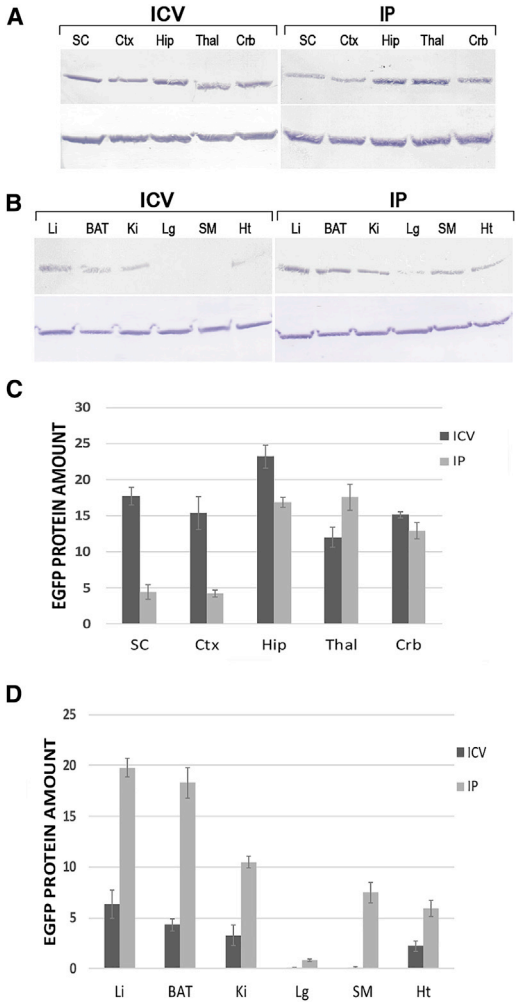


**Figure 3. Western Blot Analysis of EGFP and β-Tubulin Protein Levels in CNS and Peripheral Organs after Intrauterine Injection of rAAV9-EGFP into E14–E15 Mouse Embryos**

(A and C) Western blot analysis (A) and quantification (C) of EGFP expression in CNS of IU-injected mice. The highest EGFP levels were found to be in the hippocampus (23.2-fold) and spinal cord (17.7-fold) of mice that were administered i.c.v. injections. (B and D) Western blot analysis (B) and quantification (D) of EGFP levels in internal organs. The liver and BAT of mice that were administered IP injections exhibited elevated levels of EGFP (19.76-fold and 18.3-fold, respectively). SC, spinal cord; Ctx, cortex; Hip, hippocampus; Thal, thalamus; Crb, cerebellum; Li, liver; BAT, brown adipose tissue; Ki, kidney; Lg, lung; SM, skeletal muscle; Ht, heart. Data shown indicate mean ± SD, $p < 0.001$.

The ability of these vectors to express SMN protein *in vitro* was investigated by transducing human SMA fibroblasts. Immunofluorescent results showed co-localization of SMN and Coilin 2 proteins in the cytoplasm and nuclear Gem complexes of healthy and transduced cells (Figure S7A). While 3–4 Gem structures were observed in healthy fibroblasts, SMA fibroblasts lacked any Gem multiprotein. Cells transduced with ss- or scAAV9-SMN contained higher numbers of Gem structures compared with healthy and SMA fibroblasts (Figure S7A). Increased *SMN* expression was confirmed by qRT-PCR analysis (Figure S7B).

To investigate the fetal gene therapy of SMA disease, mouse embryos received rAAV9-SMN at E14.5–E15 via i.c.v. injection. Newborn pups were genotyped (Figure S8), and the live-born percentage of each group was calculated (Figure 4A). While 82.15% of injected heterozygous embryos and 82.24% of injected wild-type embryos were successfully carried to term, only 43.85% of the injected SMA embryos survived to birth (Figure 4A).

The daily monitoring of the body weight and lifespan of live-born mice was started on the first day after birth. The lifespan of mice in each group is shown on a Kaplan-Meier plot in Figure 4B. Untreated SMA subjects were found to have the lowest survival rate (median of 12) compared with wild-type controls (median = 405), and the lifespan of treated animals in both study groups was significantly increased compared to that of untreated subjects. ss- and scAAV9-SMN-treated mice increased survival by 93 (median = 63) and 171 (median = 105) days, respectively. While the lifespan increased with therapy, it was still shorter than that of wild-type animals (Figure 4B). Because untreated SMA mice cannot survive more than 14 days, we chose this cohort to compare the body weight of all groups here; however, a long-time comparison is shown in Figure 4C. In the P14 cohort, the body weight of the treated SMA pups was slightly lower than that of healthy controls (healthy controls = 5.73 ± 0.75 g; ssAAV9-SMN-treated pups = 3.5 ± 0.46 g; and scAAV9-SMN-treated pups = 4.16 ± 0.54 g, $p < 0.0001$) but was significantly higher than that of untreated SMA pups (2.61 ± 0.27 g, $p < 0.001$) (Figure 4C). Figure 4D shows the treated and untreated pups at P14. Pups in both treated groups had smaller body sizes compared to that of healthy controls; however, the scAAV9-SMN-treated pup's body size was larger than that of the ssAAV9-SMN-treated one (Figures 4C and 4D). Although, the body weight of SMA-treated mice increased slowly with age, at 1 month (P30), ss- and scAAV9-SMN-treated mice still had significantly lower weight (5.57 ± 0.8 g and 9.66 ± 0.46 g, respectively) when compared with wild-type mice (12.45 ± 0.8 g, $p < 0.00001$) (Figure 4C). Of note, the body weight of scAAV9-SMN-injected mice was closer to that of healthy wild-type mice. While treated SMA mice were distinguishable from healthy controls by smaller body size, there were no other distinctive phenotypic features.

### Expression of SMN Protein in the Spinal Cord, Brain, and Gastrocnemius (GC) Muscle in Prenatally Treated SMNΔ7 Mice

The level of SMN protein was analyzed in the spinal cord, brain, and GC muscle of prenatally treated SMA mice at P14 using western blotting and qRT-PCR. The western blot results revealed no or very low SMN protein in the brain, spinal cord, or muscles of untreated SMA mice. Prenatal administration of both ss- and scAAV9-SMN restored SMN protein expression in the brains and the spinal cords of treated SMA mice, with SMN levels exceeding those in the wild-type mice (Figures 5A and 5C). SMN protein levels in the brain and the spinal cord of treated mice showed 1.35-fold and 2.85-fold increases in the

A

| | ssAAV9-hSMN | | | scAAV9-hSMN | | | PBS | | |
|---|---|---|---|---|---|---|---|---|---|
| | Embryos injected | Liveborn pups | % of Survival | Embryos injected | Liveborn pups | % of Survival | Embryos injected | Liveborn pups | % of Survival |
| Wild | 50 | 41 | 85 | 42 | 35 | 81.39 | 18 | 15 | 82.24 |
| Het | 86 | 68 | 79.06 | 84 | 71 | 84.52 | 35 | 29 | 82.15 |
| SMA | 44 | 19 | 43.18 | 39 | 16 | 41.02 | 19 | 9 | 43.85 |
| Total | 180 | 128 | 71.11 | 165 | 122 | 68.98 | 72 | 53 | 69.41 |

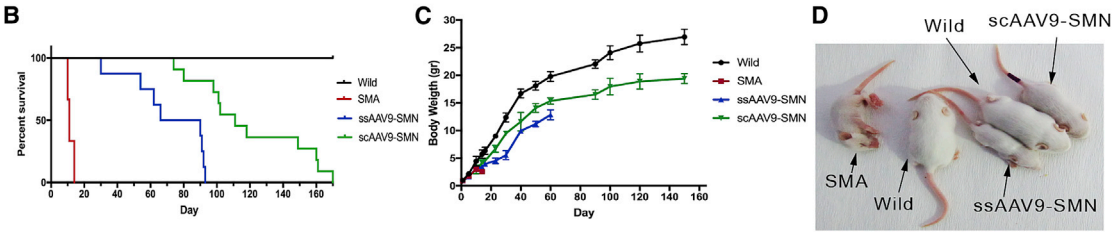


**Figure 4. Survival Rate and Body Weight of Treated and Untreated SMA Mice**

(A) The number of injected embryos and survival to birth by AAV vector. Injected SMA embryos had a lower survival rate than that of healthy embryos in all three groups. It was close to that of PBS-injected ones, which demonstrated that this increased mortality is not dependent on vector itself. (B) The lifespan of prenatally treated mice in each group was shown on a Kaplan-Meier plot (n = 10). The lifespan of treated animals in both study groups was significantly longer than that of the untreated subjects. Mice treated with scAAV9-SMN had a longer lifespan compared with ssAAV9-SMN. (C) Body weight of treated and untreated mice by age (n = 5). Although the body weight of SMA-treated pups increased slowly with age, it was still significantly less than that of healthy wild-type pups. (D) Treated and untreated pups at P14. This image clearly demonstrates the smaller body sizes of treated mice when compared with healthy wild-type pups. $p < 0.001$, by Student's unpaired two-tailed t test. Data shown indicate mean ± SD.

ssAAV9-SMN-treated group (Figure 5C) and 1.68-fold and 3.62-fold increases in the scAAV9-SMN-treated group (Figure 5C), respectively. Treated mice in the scAAV9-SMN group showed the highest amount of SMN protein in both brain and spinal cord (Figures 5A and 5C). SMN levels in the GC muscles of both treated groups did not recover to wild-type levels (0.12-fold and 0.25-fold) (Figure 5C); however, levels in the brain and spinal cord surpassed those in the wild-type counterparts. Investigation of SMN expression in different tissues by RT-PCR confirmed the western blot results. Our results showed that the highest SMN expression was achieved in spinal cord following i.c.v. administration of scAAV9-SMN (Figure 5D). Furthermore, immunofluorescent results demonstrated intensive SMN expression in lower motor neurons (anterior horn cells) of the wild-type group and both treated groups of SMA mice at P14 (Figure 6A). In comparison, a weak and scattered SMN signal was observed in untreated SMA mice. The number of motor neurons was also significantly higher in wild-type and both treated groups, with more double-positive cells observed in scAAV9-SMN treated mice (Figure 6A). The average numbers of lower motor neurons in SMA and healthy wild-type mice at P14 were 10.5 ± 1.4 and 28 ± 2.3, respectively (Figure 6B). These numbers were 18 ± 2.8 and 24.5 ± 3.4 in ss- and scAAV9-SMN-treated mice, respectively (Figure 6B). In addition to SMN recovery in both treated groups, mice treated with scAAV9-SMN also showed improved the morphology of motor neuron cells (Figure 6B). To investigate the muscle morphology of mice in each group, the GC muscles of mice euthanized at P14 were removed and paraffin embedded, followed by a day of fixation in 4% paraformaldehyde (PFA) at 4°C. Muscles were then cut to a 5-μm thickness and stained with H&E and analyzed under light microscopy. As demonstrated in Figure 6C, while the GC muscle of SMA mice was totally atrophied, the muscles of both treated groups were found to have rescued morphology. This indicates that even a very low level of *SMN* gene expression, such as that seen in the muscle of i.c.v.-injected mice, was enough to prevent muscle atrophy.

## DISCUSSION

With recent advances in fetal genome analysis, physicians can detect genetic abnormalities before birth. Early detection allows for treatment plan implementation prenatally or shortly after birth, potentially leading to the best possible outcomes. Technological advances in prenatal screening tests combined with breakthroughs in gene delivery have paved the way for fetal gene therapy studies. Many recent publications demonstrate the intriguing potential of this approach for clinical usage.[17–21]

For many lethal neurodegenerative disorders such as SMA, fetal gene therapy is an ideal approach. Symptoms of the most severe forms of SMA (types 0 and I) appear from the late prenatal period to the early postnatal period.[4–6] Martínez-Hernández et al.[22] reported a prenatal delay of muscle maturation in SMA that emphasizes the importance of initiating treatment as early as possible. Therefore, we investigated the applicability of fetal gene therapy for the prevention of SMA symptoms using a mouse model. Because clinical trials have already demonstrated the safety and efficiency of AAV vectors in young children with SMA,[13,23] we decided to use this vector for gene transfer into mouse embryos. Our results show that an i.c.v. injection of rAAV9-EGFP leads to a wider spread of transgene expression in the target CNS cells, especially motor neurons in the spinal cord (Figures 1 and 3). Therefore, we used the i.c.v. injection route for AAV9-SMN administration in mouse embryos.

In this study, a single dose of 4E+10 vector genome copy (vgc) of either ssAAV9-SMN or scAAV9-SMN administered via i.c.v.

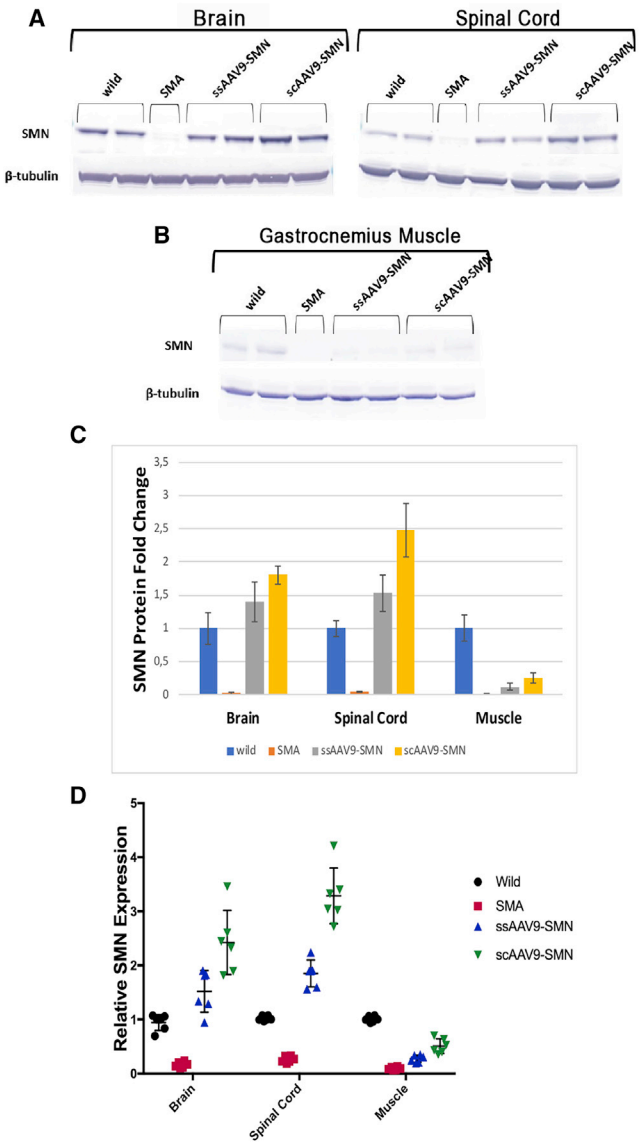


**Figure 5. Western Blot and qRT-PCR Analysis of SMN Expression Levels on P30 in Brain, Spinal Cord, and Muscle of the AAV9-SMN-Injected SMA Mice and PBS-Injected Controls**

(A and B) SMN protein levels in (A) brain and spinal cord and (B) gastrocnemius muscle. (C) Values for each sample were normalized to β-tubulin protein levels. Data shown indicate mean ± SD. (D) qRT-PCR results. SMN expression levels in each sample were normalized to GAPDH expression levels as a housekeeping gene; then relative expressions to wild-type samples were calculated. The fold changes of SMN expression in the brain, spinal cord, and muscles of ssAAV9-SMN-treated mice were 1.57-fold ± 0.38-fold, 1.89-fold ± 0.25-fold, and 0.27-fold ± 0.06-fold, respectively. For scAAV9-SMN-treated mice, it was found to be 2.4-fold ± 0.6-fold, 3.2-fold ± 0.51-fold, and 0.47-fold ± 0.13-fold, respectively. $p < 0.001$ for brain and spinal cord results, and $p < 0.01$ for muscle results.

injection resulted in an increased lifespan in treated SMA mice; 60 ± 23 and 105 ± 50 days, respectively (Figure 4C). The longer lifespans of scAAV-injected mice suggest that scAAV has higher efficacy than ssAAV *in vivo*. These results are consistent with those of Wu et al.[24] The decreased efficiency of ssAAV derives from relaying this virus to the host cells to synthesize double-stranded DNA from the ssDNA genome, and this step differs from cell type to cell type.[25] Furthermore, the greater stability of the double-stranded DNA of scAAV over the ssDNA of ssAAV results in more durable gene expression for a longer time.[26] Early postnatal gene therapy experiments on various SMA mouse models have led to an increased lifespan while partially reducing disease symptoms.[10–12] We aimed to investigate the possibility and efficacy of *in utero* delivery of AAV-SMN vectors for preventing disease manifestations. This is the first time for investigating fetal gene delivery using the AAV vector for SMA and direct point-by-point comparison of the results of this study with those of previous postnatal studies is challenging, due to dissimilarities in the administration route, dosage levels, and developmental stage. Not only vector doses and transgene cassette, but also environmental conditions can cause differences in the lifespans of treated mice.[27] Butchbach et al. showed that the maternal diet could also affect the lifespan of SMA mice.[27] They reported up to 25% increase in the lifespan of SMA littermates of *Smn*−/+, *SMN2*+/+, and *SMN2Δ7*+/+ females when fed with prepared food containing 5.2% lipid and 22.6% protein,[27] which varies from food used in our study (3% lipid and 28% protein).

Consistent with previous postnatal studies,[12,28,29] i.c.v. injection led to the biodistribution of rAAV9 into peripheral organs (Figure 3). In our study, similar to the results of Armbruster et al.,[12] skeletal muscles following i.c.v. injection had a very slight increase in the expression of SMN protein (Figure 5). Muscle phenotype and integrity were rescued in both treated groups (Figure 6C). Untreated SMA mice, however, showed small, rounded, atrophic fibers (Figure 6C). These results are consistent with the results of Glascock et al.[30] According to previous studies, meager amounts of SMN protein are sufficient for the normal function of muscles.[12,31] It has been reported by Armbruster et al.[12] that the i.c.v. injection of scAAV9-SMN1 is sufficient for the improvement of disease symptoms of the SMA disease in SMNΔ7 mouse model, whereas concomitant use of i.c.v. and intravenous (i.v.) injections has been reported to have no increased efficacy in terms of muscle and cardiac healing criteria, contrary to anticipation. Different factors—such as the glia transduction (Figure S5) and AAV distribution via axons into blood circulation,[28,29] tissue specificity of rAAV9 tropism, the drainage of CSF into the lymph system,[32,33] intracellular barriers,[34] or tissue-specific gene regulation mechanisms[35]—may affect the transgene expression profile in different tissues. The efficient transduction of the spinal cord after i.c.v. injection (Figures 1C and 2C) demonstrated that AAV9 is a excellent candidate for fetal gene therapy of SMA. However, our findings demonstrate that rAAV9 vectors have a higher tropism to the hippocampus (in i.c.v. and IP groups) and the thalamus (in the IP group) when compared to other brain regions (Figures 3A and 3C). This broader distribution of AAV9 vectors in the brain and spinal cord may be due to a higher ratio of surface area exposed to the CSF containing AAV9 vectors.[32]

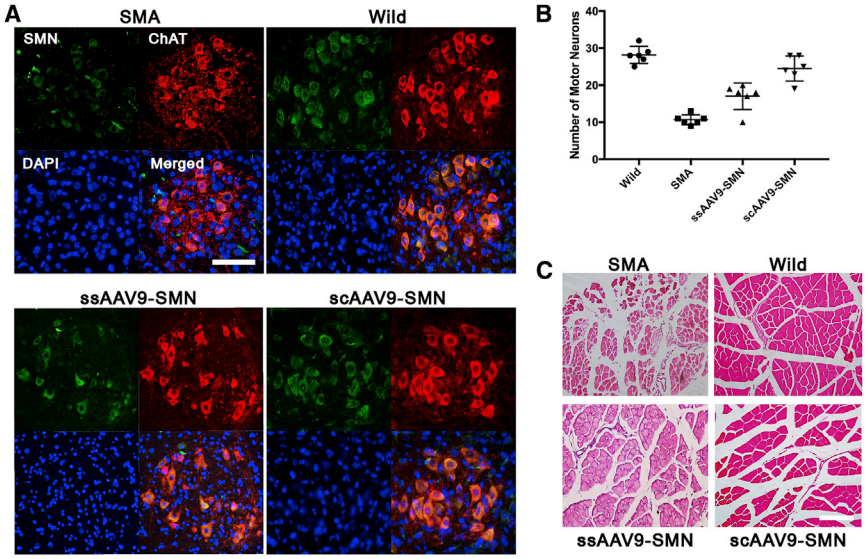


**Figure 6. Prenatal Treatment of SMA Embryos with rAAV9-SMN Rescued Motor Neuron Loss and Prevented Muscle Atrophy at P14**

(A) Motor neurons in the anterior horn of the spinal cords. Untreated SMA mice demonstrated the scattered and weak SMN signal in motor neurons compared with wild-type and treated ones. (B) The numbers of motor neurons in the spinal cord of both the ssAAV-SMN1- and scAAV9-SMN-treated groups were significantly more than that in the untreated SMA group (means ± SD were 18 ± 2.8 and 24.5 ± 3.4 compared with 10.5 ± 1.4, respectively). There was not a significant difference between number of motor neurons in scAAV9-SMN-treated mice and healthy wild-type mice (means ± SD were 24.5 ± 3.4 and 28 ± 2.3, respectively), n = 6. (C) Histology of GC muscles in each group. SMA mice demonstrated totally atrophied muscles made of tiny, scattered, and round muscle fibers. The muscle integrity in both treated groups was rescued. Muscle fibers in ssAAV-SMN1-treated mice still remained smaller and showed a round phenotype, but muscle fibers in scAAV9-SMN-treated mice were found to have a phenotype closer to that of wild-type mice. $p < 0.001$ by Student's unpaired two-tailed t test. Data shown indicate mean ± SD.

Previous studies have demonstrated significant differences in transgene expression patterns of various cell types of CNS when comparing the prenatal and postnatal administration of AAV9 via the i.v. injection route. The prenatal delivery of AAV9 causes a predominant transduction of neurons and motor neurons, which contrasts with the higher astrocyte transduction found in postnatal administration.[36] Similar to a study conducted by Rahim et al.,[36] *in utero* adminstration of scAAV9 via both i.c.v. and IP injection routes led to significant transducing of neuron cells in brain and spinal cord (Figure 2). However, we detected higher numbers of astrocytes transduced with AAV9 in the brain and spinal cord of mice that received IP injections compared to ones that received i.c.v. injections (Figure S5). In contrast to the previous study that no neural stem cell transduction was demonstrated in the subventricular zone (SVZ) from either prenatally or neonatally injected mice,[36] we detected Nestin-positive cells transduced by AAV9 in the SVZ of mice that received i.c.v. and IP injections (Figure S6). The large numbers of neural stem cells (NSCs) and progenitor cells in the SVZ[37] make them a tantalizing target for gene therapy of CNS disorders. Here, for the first time, we demonstrated some evidence of SVZ-NSC transduction by the AAV9 vector after i.c.v. or IP injection (Figures S6A–S6C). Targeting NSC and long-time transgene expression in these cells is considered to be the most significant advantage to fetal gene therapy. However, more experiments are necessary using highly sensitive methods such as laser capturing of NSCs, isolating them via flow cytometry, and single-cell qRT-PCR to determine the type and percentage of the transduced NSCs (quiescent NSCs [qNSCs] and active NSCs [aNSCs]) along with the duration of transgene expression.

While SMA mice had a reduced number of motor neurons in the anterior part of the spinal cord (lower motor neuron), these numbers increased in both treated SMA groups and resembled that of normal healthy mice (Figure 6A). The number and morphology of motor neurons in scAAV9-treated mice completely resemble that of healthy mice, reflecting results from previous studies.[12,38] However, in contrast to the improvements in disease symptoms, all treated mice remained smaller in size when compared to their healthy counterparts (Figures 4C and 4D). These results are consistent with the postnatal gene therapy study results determined by Armbruster et al.[12] Surprisingly, the tail and ear tissue necrosis detected in previous postnatal SMA gene therapy studies[12,39,40] was not detected in any of the treated mice in this study. Unfortunately, the main cause of necrosis in SMA subjects is still unknown. Previous studies reported distal necrosis in SMA type I infants with severe vascular perfusion abnormalities.[41] Moreover, a "thinning of the basement membrane" of small arterial vessels in SMA patient muscle was reported.[42] Meanwhile, there is a close similarity between vascularization and innervation patterns in the body. Also, these two systems have an integral and codependent relationship in motor neuron diseases. Therefore, another group hypothesized that autonomic dysfunction could be the main cause of vasculopathy in SMA.[43] In preclinical studies, tail and ear necrosis were observed in treated mice with significantly extended survival,[39,40] Hua et al.[44] demonstrated that a single embryonic i.c.v. injection of antisense oligonucleotide (ASO) can rescue tail and ear necrosis in SMA type III mice, which is similar to our results after the administration of AAV9-SMN via i.c.v. injection. In contrast, they showed that infusion of the same ASO via i.c.v. injection into the neonatal mice was insufficient to prevent tail and ear necrosis and solely delayed the onset for 2 weeks.[44] They concluded that skeletal muscle denervation and vascular necrosis are likely main causes of distal necrosis.[44]

In this study, IU administration of AAV9 via i.c.v. injection did cause an increase in the abortion rate of SMA mice compared with that for healthy embryos (Figure 4A). The hemorrhages were seen in the brains

of aborted SMA mice that received i.c.v. injections. Unlike tail and ear necrosis, brain hemorrhage can happen immediately after i.c.v. injection, which may be due to the impairment or fragility of vascular endothelial cells in SMA mice that makes embryos more susceptible to complications of i.c.v. injection and increases the risk of abortion. Although the AAV vectors are harmless and safe, some inflammatory or toxic reaction against the rAAV capsid or transgenic product cannot be ruled out.[45–47] According to Haddad et al.,[48] the lipopolysaccharides and other endotoxin contamination that remain in the final rAAV product, as well as the production and purification protocols, may be other possible malefactors for the increased mortality rate.[48] However, here, healthy embryos that received *in utero* rAAV or PBS demonstrated similar survival rates (Figures 1B and 4A). Thus, the possible endotoxin toxicity explanation is weak. Taking into consideration all these findings, as well as the results from Foust et al.,[39] we believe the most likely cause of brain bleeding in injected SMA embryos to be vascular disorders. Since SMA is a multi-system disorder affecting internal organs as well as lower motor neurons,[49] systemic delivery of therapeutic agents via i.v. injection could raise the advantage of transducing different cells and tissues. However, due to the vascular abnormalities in SMA, special care needs to be considered while performing i.v. injection via vitelline vessels in mouse embryos, which can be even more challenging compared to i.v. injection in the embryos of larger animals such as pigs or nonhuman primates (NHPs).

Consequently, here, for the first time, we demonstrated that fetal gene therapy using AAV9 could alleviate disease symptoms and increase the lifespan of treated SMA mice. Ear and tail tissue necrosis seen in previous postnatal gene therapy studies were not detected in any of the treated mice in this study. However, one factor that requires further evaluation is the amount of the viral vector spillages into maternal blood circulation, likely leading to maternal germline transduction or the development of an immune response to viral vector. Mattar et al.[50] demonstrated the transduction of maternal liver, ovary, and other peripheral organs following *in utero* administration of scAAV vectors in NHPs. An immune response against the AAV vector capsids was detected in all mothers. However, no maternal germline (oocyte) transduction was detected in the study of NHPs, which keeps hopes high for the potential application of *in utero* gene therapy in the future.[50] Additionally, before fetal gene therapy can be allowed to reach its full potential in the clinical setting, other issues also need to be addressed, ranging from ethical to cultural and protocols provided. However, time is of the essence. Advances in prenatal diagnostic technologies and clinical trials have demonstrated the safety of AAV-mediated gene therapy in SMA subjects,[13] and the U.S. Food and Drug Administration (FDA) has approved the two AAV-based gene therapies for human treatment.[15,51] It is time to consider the benefits and move forward with fetal gene therapy to reveal its true potential for patient benefits.

## MATERIALS AND METHODS

### Preparation of rAAV9 Vectors

All rAAV9 vectors used in this study were produced at the Gao lab, Horae Gene Therapy Center, University of Massachusetts Medical School, Worcester, MA, USA.[16] All rAAV vectors were produced by triple transfection of a *cis*-plasmid containing the rAAV-containing transgene cassette and AAV2 inverted terminal repeats, a *trans*-plasmid containing the AAV2 *rep* gene and AAV9 *cap* gene, and a pDF6 adeno helper plasmid in HEK293 cells. Isolated scAAV9-EGFP, ssAAV9-hSMN1, and scAAV9-hSMN1 vectors were purified using cesium chloride gradient centrifugation and then desalted by dialysis. The titration of purified rAAV genome copy number was assessed using Taqman Real-Time qPCR. The vector purity was assessed by silver staining to visualize the viral protein (VP)1, VP2, and VP3.[16]

### Animals

All animal procedures were approved by the Ege University Local Ethics Committee for Animal Experimentation (process number: 2014-019), Izmir, Turkey. All experiments conform to all relevant regulatory standards. Animals were housed in isolated cages with open access to water and food. Cages were maintained in a controlled animal facility with 50% humidity at 22°C, with a 12-h/12-h light-dark cycle. All animals were monitored daily for health.

The 005025 SMAΔ7 breeding (*Smn*+/−, *SMN2*+/+, and *SMNΔ7*+/+) mice pairs were purchased from Jackson Laboratory, Bar Harbor, ME, USA. The healthy wild-type (*Smn*+/+, *SMN2*+/+, and *SMNΔ7*+/+) female and male mice, the offspring of 005025 SMAΔ7 mice, were used for the biodistribution study of rAAV9-EGFP. Heterozygote pairs were allowed to breed, with pregnant females then being used for fetal gene therapy study.

### *In Utero* Administration of rAAV9 Vectors

Mice were allowed to breed, and the date of vaginal plug formation was recorded as day 1 of gestation. At day 15, pregnant mice were anesthetized using isoflurane inhalation (2% isoflurane + 6% oxygen), and then, to reach the uterine horns, a 2-cm midline laparotomy was performed. Mice received 2 mg/kg meloxicam via subcutaneous injection prior to surgery.

For biodistribution study, a total of 52 fetuses (male and female) underwent IU injection on E15. 21 fetuses received 2 μL (4E+10 vgc) and 19 fetuses received 5 μL (1E+11 vgc) scAAV9-EGFP via i.c.v. and IP injections, respectively. 12 fetuses were injected with PBS as a control. To conduct fetal gene therapy for SMA, male and female mice that were heterozygotes for the *Smn* gene (*Smn*+/−, *SMN2*+/+, and *SMNΔ7*+/+) were allowed to mate. 2 μL (4E+10 vgc) rAAV9-SMN was delivered prenatally into the brains of the embryonic mice via i.c.v. injection into one of the lateral ventricles (LVs). All embryos per dam were treated with ssAAV9-SMN or with scAAV9-SMN vector. The genotype screening of newborn pups was performed immediately following birth, and homozygous mutant, heterozygous, and wild-type pups were separated. For control groups, all embryos from separate dams were injected with PBS and genotyped after birth. From a total of 417 embryos that underwent i.c.v. injection, 180 embryos received ssAAV9-SMN and 165 embryos received scAAV9-SMN at E14–E15. All injections were performed using sterile 34G

Hamilton needles at a rate of 1 μL/10 s. A moist environment was attained during surgery by constantly wetting down fetuses using warmed PBS solution. Following the surgery, the abdominal cavity was filled with 1 mL PBS containing cefazolin (100 mg/kg), and the incision was then closed using 0.5 absorbable suture. A Deltaphase Isothermal Pad (Braintree Scientific, Braintree, MA, USA) was used to prevent hypothermia during surgery. Post-surgery, mice were placed in separate cages and kept warm for more than 1 h until the effects of the anesthetic dissipated. To prevent pain, meloxicam (1.5 mg/kg) was added to drinking water for 3 days, and mice were monitored daily through to vaginal delivery. Treated and untreated pups were weaned until 21 days of age; then their growth and health were continually monitored into adulthood.

#### GFP Imaging of Living Animals

Newborn pups were monitored at P1 and P14 for EGFP expression in brain and spinal cord using the IVIS spectrum imaging system (Caliper Life Sciences, Hopkinton, MA, USA) under isoflurane inhalational anesthesia. Excitation and emission spectra of 465 nm and 560 nm wavelengths, respectively, were used for the detection of GFP fluorescence using a GFP-specific emission filter and an exposure time of 0.2 s. Images were captured and analyzed automatically using the Living Image program, v4.5.2.

#### Tissue Preparation for Immunofluorescence

The newborn pups were kept with their mothers in the same cage until P30, when they were euthanized for further analysis. Deeply anesthetized mice (ketamine/xylazine, 250/150 mg/kg, intraperitoneally [i.p.]) were perfused transcardially with 25 mL 1× PBS containing 25,000 U/L heparin. This was followed by a fixation using 25 mL 4% PFA fixation solution. Then the brain and the spinal cord were extracted and postfixed in 4% PFA for 2 days. Following the washing of PFA from tissue using PBS in 4°C for several hours, tissues were cryoprotected in 30% sucrose in 4°C until they sank. Thereafter, tissues were embedded in O.C.T. Tissue-Tek Compound (Sakura Finetek, Torrance, CA, USA) and frozen immediately in liquid nitrogen. 15-μm floating sections were then cut using cryostat (Microm HM 560 Cryostat, Thermo Fisher Scientific, Waldorf, Germany).

#### Immunofluorescence Analysis of Tissue Sections

The tissue sections were incubated with 1/1,000 diluted rabbit anti-GFP antibody (Abcam, ab6556, Cambridge, MA, USA), 1/250 diluted goat anti-GFAP (Abcam, ab53554), 1/500 diluted rabbit anti-NeuN (Abcam, ab104225, Cambridge, MA, USA), 1/50 diluted goat anti-ChAT (EMD Millipore, AB144P, Billerica, MA, USA), or 1/200 diluted monoclonal mouse anti-SMN (EMD Millipore, Clone 2B1, Billerica, MA, USA) primary antibodies at 4°C for 24 h. The following day, tissue sections were washed three times with PBS containing 1% Triton X-100 and 0.5% Tween 20 for 30 min. Sections were incubated in the following antibodies (1/500 diluted): goat anti-rabbit Alexa Fluor 488 (Abcam, ab150081, Cambridge, MA, USA), goat anti-rabbit Alexa Fluor 594 (Abcam, ab150084, Cambridge, MA, USA), donkey anti-goat Alexa Fluor 594 (Abcam, ab150140, Cambridge, MA, USA), goat anti-mouse Alexa Fluor 568 (Thermo Scientific, Rockford, IL, USA), or goat anti-mouse Alexa Fluor 488 (Abcam, Cambridge, MA, USA) secondary antibodies at 4°C for 24 h. After washing, sections were mounted with Vectashield mounting media (DAPI; Vector Laboratories, Burlingame, CA, USA) containing 4',6-diamidino-2-phenylindole and analyzed using Olympus fluorescent microscopy (Olympus, Tokyo, Japan). For quantification of neurons expressed EGFP in 4 separate images from each mouse, the number of cells reflecting GFP were counted three times using the naked eye.

#### Quantitative Real-Time PCR Analysis

Approximately 50 mg of each tissue was flash-frozen in liquid nitrogen immediately after harvesting and stored at −80°C until it could be processed. Total RNA was isolated by TRIzol (Thermo Fisher Scientific, 15596018, Bleiswijk, the Netherlands) with DNase I treatment, and 1 μg total RNA was used as a template for the synthesis of cDNA via the Transcriptor First Strand cDNA Synthesis Kit (Roche Diagnostics, Indianapolis, IN, USA). 2.5 μL cDNA was subjected to RT-PCR reaction using the TaqMan Gene Expression Assays Kit (Thermo Fisher Scientific, Bleiswijk, the Netherlands) containing primers and a probe specific to *SMN1* gene[52] to quantify related cDNA according to the manufacturer's protocol. Internal control of qRT-PCR in mouse samples was achieved by detecting mouse glyceraldehyde 3-phosphate dehydrogenase (*Mm-Gapdh*) gene expression using a TaqMan gene expression kit containing primers and a probe for *Mm-Gapdh* gene (Thermo Fisher Scientific, 4331182, Bleiswijk, the Netherlands). The LightCycler h-G6PDH Housekeeping Gene Set (Roche Applied Science, 03261883001, Penzberg, Germany) was used as the qRT-PCR's internal control in human fibroblasts. The following program was used for all the RT-PCR analysis; 1 cycle denaturation in 95°C for 10 min, 50 cycles of 94°C for 10 s following 60°C for 1 min, and 1 cycle cooling in 40°C. SMN expression was normalized to the housekeeping gene, and then data were analyzed by the delta-delta- $C_T$ ($2^{-\Delta\Delta CT}$) algorithm to calculate relative gene expression.

#### Western Blot

Tissues were homogenized in ice-cold radioimmunoprecipitation assay (RIPA) lysis buffer (Thermo Fisher Scientific, 89900, Bleiswijk, the Netherlands) containing protease inhibitor cocktail (Roche Applied Science, Penzberg, Germany) in accordance with the manufacturer's protocol. The protein concentration of each sample was detected using the Pierce BCA Protein Assay Kit (Thermo Fisher Scientific, Bleiswijk, the Netherlands) in accordance with the manufacturer's protocols. Equal amounts of protein samples (25 μg) were added to each well of 4%–12% Bis-Tris SDS-PAGE protein gels (Novex, Invitrogen, Waltham, MA, USA). Separated proteins on the gel were transferred onto a polyvinylidene difluoride (PVDF) membrane using the iBlot Gel Transfer System (Invitrogen, Waltham, MA, USA). The blocked and washed membrane was then exposed to 1/3,000 diluted rabbit anti-EGFP antibody (Abcam, ab6556, Cambridge, MA), 1/1,000 diluted anti-SMN (EMD Millipore, Clone 2B1, 05-1532, Billerica, MA, USA), or 1:2,000 diluted anti-β-tubulin monoclonal antibody (Thermo Fisher Scientific, BT7R, Bleiswijk, the Netherlands) and then incubated 1 h at room temperature (RT). The

anti-mouse Western Breeze Chromogenic Immunodetection Kit (Novex, WB7103, Invitrogen, Waltham, MA, USA) containing ready-to-use alkaline-phosphatase-conjugated anti-mouse secondary antibody was used for chromogenic detection of the EGFP and β-tubulin proteins. Quantification of western blot results was achieved using the ImageJ program (https://imagej.nih.gov/ij/).

### Calculating the Lifespan and the Body Weight of Injected Mice

The injected mice were monitored daily, and their body weights were measured. A number of untreated SMA, IU-treated SMA, and healthy wild-type siblings were chosen randomly, and lifespans of treated and untreated mice were compared. At the end of the study, the averages of all the values in each group were calculated, and a graphic was created.

### Statistical Analysis

All the results are shown as mean ± SD. Experimental data were analyzed via Student's unpaired two-tailed t test using SPSS 15.0 software (Chicago, IL, USA), and a p value less than 0.05 was considered to be significant. All experiments were repeated at least three times.

## SUPPLEMENTAL INFORMATION

Supplemental Information can be found online at https://doi.org/10.1016/j.ymthe.2019.08.017.

## AUTHOR CONTRIBUTIONS

Conceptualization, F.O., G.G., and A.R.; Methodology, A.R. and G.A.C.; Investigation, A.R., G.A.C., C.G., M.B., B.D., A.A., and Q.S.; Resources, F.O., H.O., C.G., and G.G.; Writing – Original Draft, A.R.; Review & Editing, F.O. and G.G.; Visualization, A.R. and G.A.C.; Supervision, F.O. and G.G.; Project Administration: A.R.; Funding Acquisition, F.O. and G.G.

## CONFLICTS OF INTEREST

G.G. is a scientific co-founder of Voyager Therapeutics and holds equity in the company. G.G. is an inventor on patents with potential royalties licensed to Voyager Therapeutics and other biopharmaceutical companies.

## ACKNOWLEDGMENTS

This work is supported by a grant from the Ege University Scientific Research Projects (APAK, grant number 2014/TIP/083) to F.O. and by NIH grant R01NS076991-01 to G.G.

## REFERENCES

1. Verhaart, I.E.C., Robertson, A., Wilson, I.J., Aartsma-Rus, A., Cameron, S., Jones, C.C., Cook, S.F., and Lochmüller, H. (2017). Prevalence, incidence and carrier frequency of 5q-linked spinal muscular atrophy – a literature review. Orphanet J. Rare Dis. *12*, 124.
2. Farrell, P.M. (2008). The prevalence of cystic fibrosis in the European Union. J. Cyst. Fibros. *7*, 450–453.
3. Pearn, J. (1980). Classification of spinal muscular atrophies. Lancet *1*, 919–922.
4. Grotto, S., Cuisset, J.M., Marret, S., Drunat, S., Faure, P., Audebert-Bellanger, S., Desguerre, I., Flurin, V., Grebille, A.G., Guerrot, A.M., et al. (2016). Type 0 spinal muscular atrophy: further delineation of prenatal and postnatal features in 16 patients. J. Neuromuscul. Dis. *3*, 487–495.
5. Al Dakhoul, S. (2017). Very severe spinal muscular atrophy (type 0). Avicenna J. Med. *7*, 32–33.
6. Shababi, M., Lorson, C.L., and Rudnik-Schöneborn, S.S. (2014). Spinal muscular atrophy: a motor neuron disorder or a multi-organ disease? J. Anat. *224*, 15–28.
7. Rahim, A.A., Buckley, S.M., Chan, J.K., Peebles, D.M., and Waddington, S.N. (2011). Perinatal gene delivery to the CNS. Ther. Deliv. *2*, 483–491.
8. Colletti, E., Lindstedt, S., Park, P.J., Almeida-Porada, G., and Porada, C.D. (2008). Early fetal gene delivery utilizes both central and peripheral mechanisms of tolerance induction. Exp. Hematol. *36*, 816–822.
9. Larson, J.E., and Cohen, J.C. (2000). In utero gene therapy. Ochsner J. *2*, 107–110.
10. Dominguez, E., Marais, T., Chatauret, N., Benkhelifa-Ziyyat, S., Duque, S., Ravassard, P., Carcenac, R., Astord, S., Pereira de Moura, A., Voit, T., and Barkats, M. (2011). Intravenous scAAV9 delivery of a codon-optimized SMN1 sequence rescues SMA mice. Hum. Mol. Genet. *20*, 681–693.
11. Meyer, K., Ferraiuolo, L., Schmelzer, L., Braun, L., McGovern, V., Likhite, S., Michels, O., Govoni, A., Fitzgerald, J., Morales, P., et al. (2015). Improving single injection CSF delivery of AAV9-mediated gene therapy for SMA: a dose-response study in mice and nonhuman primates. Mol. Ther. *23*, 477–487.
12. Armbruster, N., Lattanzi, A., Jeavons, M., Van Wittenberghe, L., Gjata, B., Marais, T., Martin, S., Vignaud, A., Voit, T., Mavilio, F., et al. (2016). Efficacy and biodistribution analysis of intracerebroventricular administration of an optimized scAAV9-SMN1 vector in a mouse model of spinal muscular atrophy. Mol. Ther. Methods Clin. Dev. *3*, 16060.
13. Mendell, J.R., Al-Zaidy, S., Shell, R., Arnold, W.D., Rodino-Klapac, L.R., Prior, T.W., Lowes, L., Alfano, L., Berry, K., Church, K., et al. (2017). Single-dose gene-replacement therapy for spinal muscular atrophy. N. Engl. J. Med. *377*, 1713–1722.
14. Al-Zaidy, S., Pickard, A.S., Kotha, K., Alfano, L.N., Lowes, L., Paul, G., Church, K., Lehman, K., Sproule, D.M., Dabbous, O., et al. (2019). Health outcomes in spinal muscular atrophy type 1 following AVXS-101 gene replacement therapy. Pediatr. Pulmonol. *54*, 179–185.
15. Hoy, S.M. (2019). Onasemnogene abeparvovec: first global approval. Drugs *79*, 1255–1262.
16. Rashnonejad, A., Chermahini, G.A., Li, S., Ozkinay, F., and Gao, G. (2016). Large-scale production of adeno-associated viral vector serotype-9 carrying the human survival motor neuron gene. Mol. Biotechnol. *58*, 30–36.
17. Massaro, G., Mattar, C.N.Z., Wong, A.M.S., Sirka, E., Buckley, S.M.K., Herbert, B.R., Karlsson, S., Perocheau, D.P., Burke, D., Heales, S., et al. (2018). Fetal gene therapy for neurodegenerative disease of infants. Nat. Med. *24*, 1317–1323.
18. Ma, H., Marti-Gutierrez, N., Park, S.W., Wu, J., Lee, Y., Suzuki, K., Koski, A., Ji, D., Hayama, T., Ahmed, R., et al. (2017). Correction of a pathogenic gene mutation in human embryos. Nature *548*, 413–419.
19. Ahmed, S.G., Waddington, S.N., Boza-Morán, M.G., and Yáñez-Muñoz, R.J. (2018). High-efficiency transduction of spinal cord motor neurons by intrauterine delivery of integration-deficient lentiviral vectors. J. Control. Release *273*, 99–107.
20. MacKenzie, T.C. (2018). Future AAVenues for in utero gene therapy. Cell Stem Cell *23*, 320–321.
21. Ricciardi, A.S., Bahal, R., Farrelly, J.S., Quijano, E., Bianchi, A.H., Luks, V.L., Putman, R., López-Giráldez, F., Coşkun, S., Song, E., et al. (2018). In utero nanoparticle delivery for site-specific genome editing. Nat. Commun. *9*, 2481.
22. Martínez-Hernández, R., Soler-Botija, C., Also, E., Alias, L., Caselles, L., Gich, I., Bernal, S., and Tizzano, E.F. (2009). The developmental pattern of myotubes in spinal muscular atrophy indicates prenatal delay of muscle maturation. J. Neuropathol. Exp. Neurol. *68*, 474–481.
23. Kay, M.A., and Nakai, H. (2003). Looking into the safety of AAV vectors. Nature *424*, 251.
24. Wu, T., Töpfer, K., Lin, S.W., Li, H., Bian, A., Zhou, X.Y., High, K.A., and Ertl, H.C. (2012). Self-complementary AAVs induce more potent transgene product-specific immune responses compared to a single-stranded genome. Mol. Ther. *20*, 572–579.

25. Nakai, H., Storm, T.A., and Kay, M.A. (2000). Recruitment of single-stranded recombinant adeno-associated virus vector genomes and intermolecular recombination are responsible for stable transduction of liver in vivo. J. Virol. *74*, 9451–9463.

26. Horowitz, E.D., Rahman, K.S., Bower, B.D., Dismuke, D.J., Falvo, M.R., Griffith, J.D., Harvey, S.C., and Asokan, A. (2013). Biophysical and ultrastructural characterization of adeno-associated virus capsid uncoating and genome release. J. Virol. *87*, 2994–3002.

27. Butchbach, M.E., Rose, F.F., Jr., Rhoades, S., Marston, J., McCrone, J.T., Sinnott, R., and Lorson, C.L. (2010). Effect of diet on the survival and phenotype of a mouse model for spinal muscular atrophy. Biochem. Biophys. Res. Commun. *391*, 835–840.

28. Hordeaux, J., Dubreil, L., Deniaud, J., Iacobelli, F., Moreau, S., Ledevin, M., Le Guiner, C., Blouin, V., Le Duff, J., Mendes-Madeira, A., et al. (2015). Efficient central nervous system AAVrh10-mediated intrathecal gene transfer in adult and neonate rats. Gene Ther. *22*, 316–324.

29. Schuster, D.J., Dykstra, J.A., Riedl, M.S., Kitto, K.F., Belur, L.R., McIvor, R.S., Elde, R.P., Fairbanks, C.A., and Vulchanova, L. (2014). Biodistribution of adeno-associated virus serotype 9 (AAV9) vector after intrathecal and intravenous delivery in mouse. Front. Neuroanat. *8*, 42.

30. Glascock, J.J., Shababi, M., Wetz, M.J., Krogman, M.M., and Lorson, C.L. (2012). Direct central nervous system delivery provides enhanced protection following vector mediated gene replacement in a severe model of spinal muscular atrophy. Biochem. Biophys. Res. Commun. *417*, 376–381.

31. Iyer, C.C., McGovern, V.L., Murray, J.D., Gombash, S.E., Zaworski, P.G., Foust, K.D., Janssen, P.M., and Burghes, A.H. (2015). Low levels of Survival Motor Neuron protein are sufficient for normal muscle function in the SMNΔ7 mouse model of SMA. Hum. Mol. Genet. *24*, 6160–6173.

32. Guo, Y., Wang, D., Qiao, T., Yang, C., Su, Q., Gao, G., and Xu, Z. (2016). A single injection of recombinant adeno-associated virus into the lumbar cistern delivers transgene expression throughout the whole spinal cord. Mol. Neurobiol. *53*, 3235–3248.

33. Johnston, M., and Papaiconomou, C. (2002). Cerebrospinal fluid transport: a lymphatic perspective. News Physiol. Sci. *17*, 227–230.

34. Nonnenmacher, M., and Weber, T. (2012). Intracellular transport of recombinant adeno-associated virus vectors. Gene Ther. *19*, 649–658.

35. Liu, B., Paton, J.F., and Kasparov, S. (2008). Viral vectors based on bidirectional cell-specific mammalian promoters and transcriptional amplification strategy for use in vitro and in vivo. BMC Biotechnol. *8*, 49.

36. Rahim, A.A., Wong, A.M., Hoefer, K., Buckley, S.M., Mattar, C.N., Cheng, S.H., Chan, J.K., Cooper, J.D., and Waddington, S.N. (2011). Intravenous administration of AAV2/9 to the fetal and neonatal mouse leads to differential targeting of CNS cell types and extensive transduction of the nervous system. FASEB J. *25*, 3505–3518.

37. Daynac, M., Morizur, L., Chicheportiche, A., Mouthon, M.A., and Boussin, F.D. (2016). Age-related neurogenesis decline in the subventricular zone is associated with specific cell cycle regulation changes in activated neural stem cells. Sci. Rep. *6*, 21505.

38. Passini, M.A., Bu, J., Roskelley, E.M., Richards, A.M., Sardi, S.P., O'Riordan, C.R., Klinger, K.W., Shihabuddin, L.S., and Cheng, S.H. (2010). CNS-targeted gene therapy improves survival and motor function in a mouse model of spinal muscular atrophy. J. Clin. Invest. *120*, 1253–1264.

39. Foust, K.D., Wang, X., McGovern, V.L., Braun, L., Bevan, A.K., Haidet, A.M., Le, T.T., Morales, P.R., Rich, M.M., Burghes, A.H., and Kaspar, B.K. (2010). Rescue of the spinal muscular atrophy phenotype in a mouse model by early postnatal delivery of SMN. Nat. Biotechnol. *28*, 271–274.

40. Narver, H.L., Kong, L., Burnett, B.G., Choe, D.W., Bosch-Marcé, M., Taye, A.A., Eckhaus, M.A., and Sumner, C.J. (2008). Sustained improvement of spinal muscular atrophy mice treated with trichostatin A plus nutrition. Ann. Neurol. *64*, 465–470.

41. Araujo, Ap., Araujo, M., and Swoboda, K.J. (2009). Vascular perfusion abnormalities in infants with spinal muscular atrophy. J. Pediatr. *155*, 292–294.

42. Musch, B.C., Papapetropoulos, T.A., McQueen, D.A., Hudgson, P., and Weightman, D. (1975). A comparison of the structure of small blood vessels in normal, denervated and dystrophic human muscle. J. Neurol. Sci. *26*, 221–234.

43. Arai, H., Tanabe, Y., Hachiya, Y., Otsuka, E., Kumada, S., Furushima, W., Kohyama, J., Yamashita, S., Takanashi, J., and Kohno, Y. (2005). Finger cold-induced vasodilatation, sympathetic skin response, and R-R interval variation in patients with progressive spinal muscular atrophy. J. Child Neurol. *20*, 871–875.

44. Hua, Y., Sahashi, K., Hung, G., Rigo, F., Passini, M.A., Bennett, C.F., and Krainer, A.R. (2010). Antisense correction of SMN2 splicing in the CNS rescues necrosis in a type III SMA mouse model. Genes Dev. *24*, 1634–1644.

45. Flotte, T.R., Conlon, T.J., Poirier, A., Campbell-Thompson, M., and Byrne, B.J. (2007). Preclinical characterization of a recombinant adeno-associated virus type 1-pseudotyped vector demonstrates dose-dependent injection site inflammation and dissemination of vector genomes to distant sites. Hum. Gene Ther. *18*, 245–256.

46. Salegio, E.A., Samaranch, L., Jenkins, R.W., Clarke, C.J., Lamarre, C., Beyer, J., Kells, A.P., Bringas, J., Sebastian, W.S., Richardson, R.M., et al. (2012). Safety study of adeno-associated virus serotype 2-mediated human acid sphingomyelinase expression in the nonhuman primate brain. Hum. Gene Ther. *23*, 891–902.

47. Hinderer, C., Katz, N., Buza, E.L., Dyer, C., Goode, T., Bell, P., Richman, L.K., and Wilson, J.M. (2018). Severe toxicity in nonhuman primates and piglets following high-dose intravenous administration of an adeno-associated virus vector expressing human SMN. Hum. Gene Ther. *29*, 285–298.

48. Haddad, M.R., Donsante, A., Zerfas, P., and Kaler, S.G. (2013). Fetal brain-directed AAV gene therapy results in rapid, robust, and persistent transduction of mouse choroid plexus epithelia. Mol. Ther. Nucleic Acids *2*, e101.

49. Hamilton, G., and Gillingwater, T.H. (2013). Spinal muscular atrophy: going beyond the motor neuron. Trends Mol. Med. *19*, 40–50.

50. Mattar, C.N., Nathwani, A.C., Waddington, S.N., Dighe, N., Kaeppel, C., Nowrouzi, A., Mcintosh, J., Johana, N.B., Ogden, B., Fisk, N.M., et al. (2011). Stable human FIX expression after 0.9G intrauterine gene transfer of self-complementary adeno-associated viral vector 5 and 8 in macaques. Mol. Ther. *19*, 1950–1960.

51. Smalley, E. (2017). First AAV gene therapy poised for landmark approval. Nat. Biotechnol. *35*, 998–999.

52. Rashnonejad, A., Gündüz, C., Süslüer, S.Y., Onay, H., Durmaz, B., Bandehpour, M., and Özkınay, F. (2016). In vitro gene manipulation of spinal muscular atrophy fibroblast cell line using gene-targeting fragment for restoration of SMN protein expression. Gene Ther. *23*, 10–17.

**YMTHE, Volume *27***

## Supplemental Information

# Fetal Gene Therapy Using a Single Injection of Recombinant AAV9 Rescued SMA Phenotype in Mice

**Afrooz Rashnonejad, Gholamhossein Amini Chermahini, Cumhur Gündüz, Hüseyin Onay, Ayça Aykut, Burak Durmaz, Meral Baka, Qin Su, Guangping Gao, and Ferda Özkınay**

**Supplemental Figures**

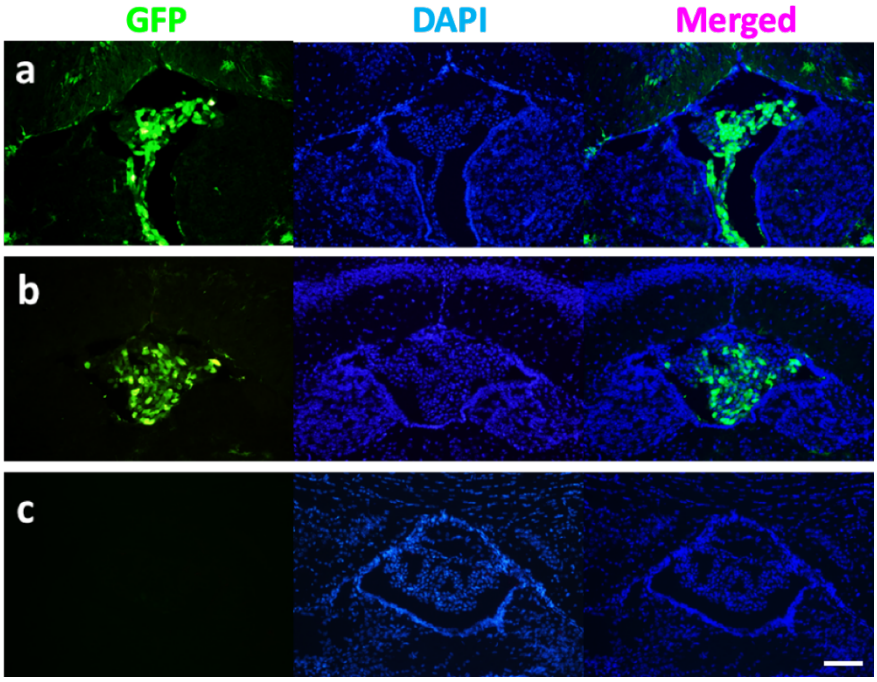


**Figure S1.** Transduction of Choroid Plexus (CP) after intrauterine administration of rAAV9-eGFP into mouse embryos at E14-15. **a**) ICV, **b**) IP, and **c**) PBS injected controls. AAV9 demonstrated strong tropism to ependymal cells in CP regions of both ICV and IP injected mice. 20X Objective, Scale bar = 100 µm.

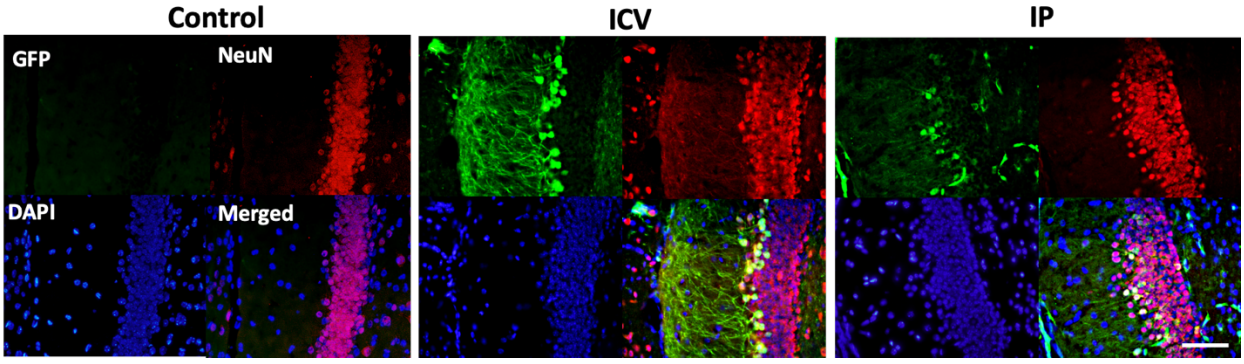


**Figure S2.** Co-expression of eGFP and NeuN proteins in the DG neurons after intrauterine administration of rAAV9-eGFP into mouse embryos at E14-15. 20X Objective, Scale bar = 100 µm.

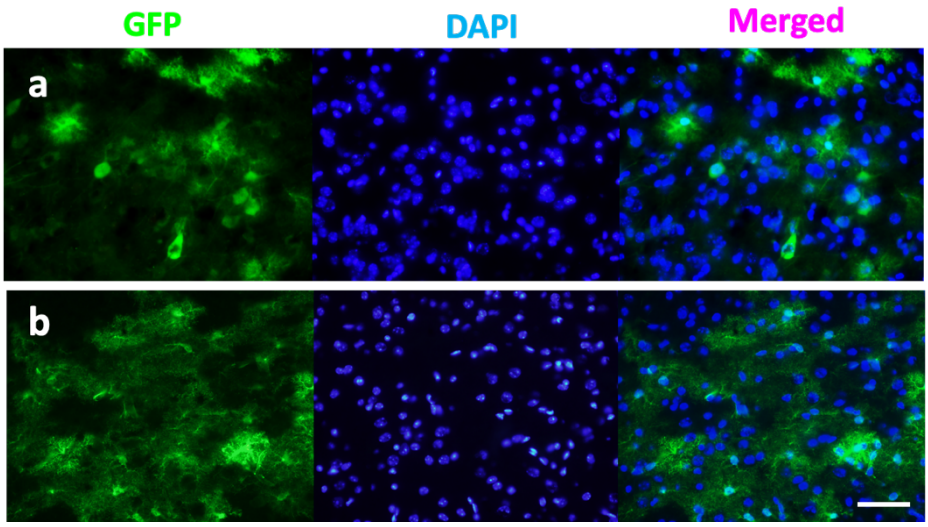


**Figure S3.** Prenatally administration of rAAV9-eGFP led to strong transduction of the cells in Thalamus; **a**) ICV, and **b**) IP injected mice. Most of the transduced cells demonstrated star-like appearance of glial cells. 40X Objective, Scale bar = 50 µm.

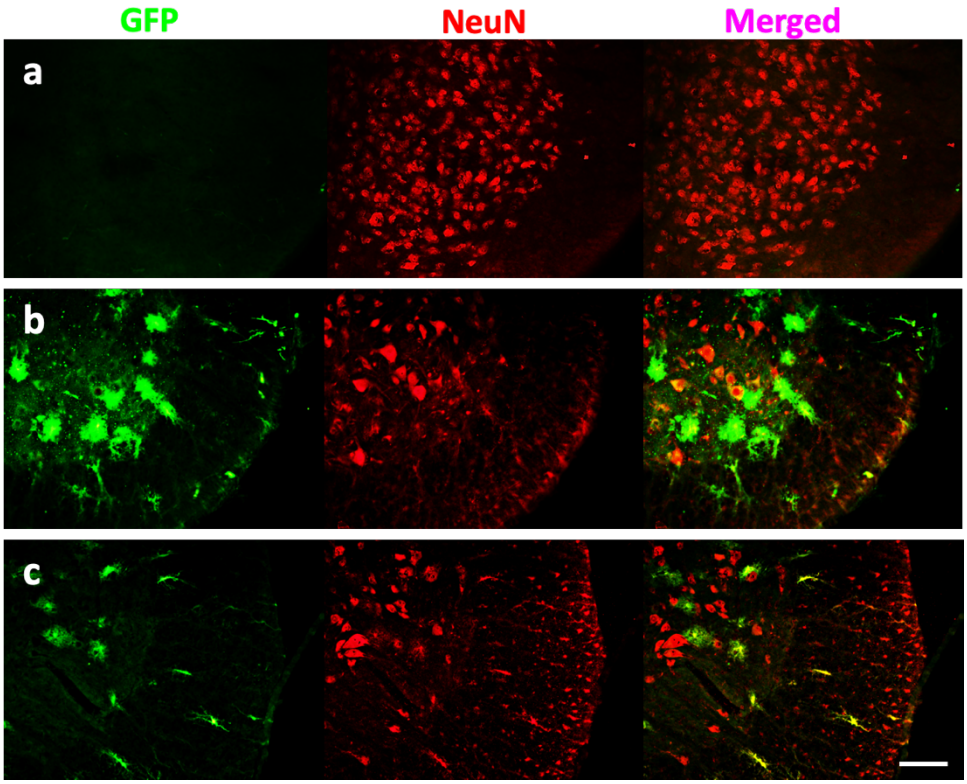


**Figure S4.** Neuronal transduction of spinal cord anterior horn cells at P30 after administration of rAAV9-GFP on E14-15. **a**) PBS, **b**) ICV, and **c**) IP 20X Objective, Scale bar = 100 µm.

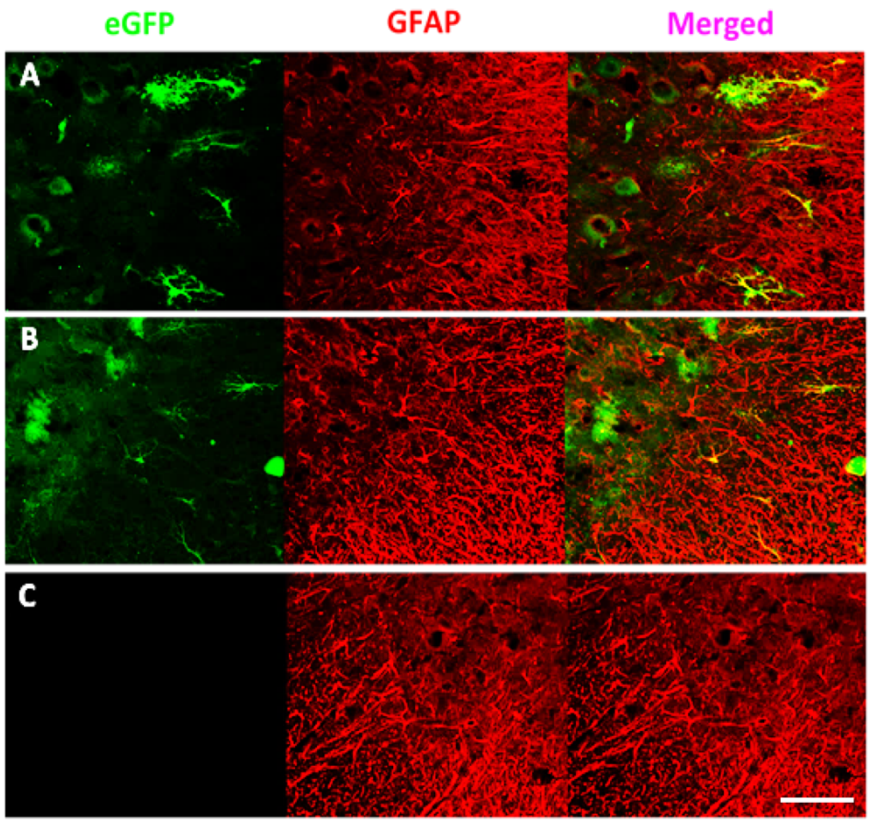


**Figure S5.** Glial transduction of mouse spinal cord at P30 after prenatal administration of rAAV9-GFP. **A**) ICV, **B**) IP, and **C**) PBS. 20X Objective, Scale bar = 100 µm.

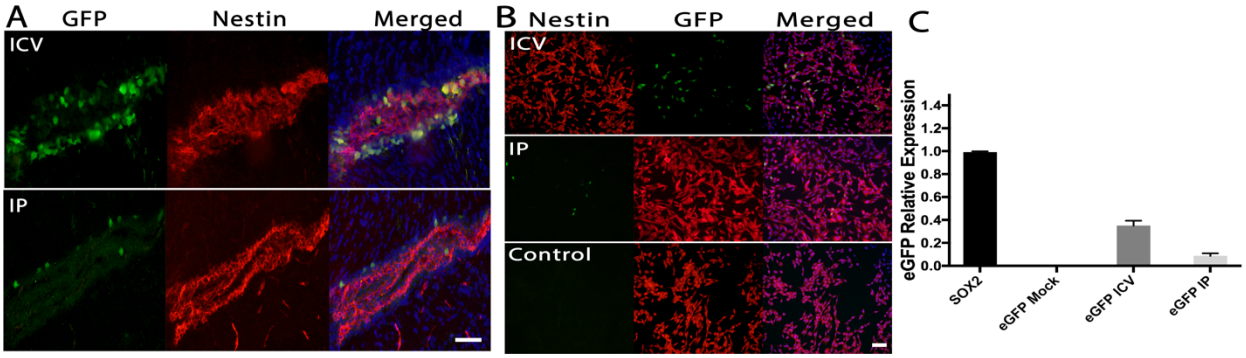


**Figure S6.** Transduction of neural stem cells in prenatally injected pups at P30. **A**) The schematic diagram of NSC localization in SVZ. **B**) Transduced Nestin positive cells located in the SVZ regions. The number of transduced NSCs in ICV injected mice is higher than those of IP injected ones. **C**) eGFP expressing NSCs were isolated from SVZ regions of injected mouse brains. **D**) eGFP relative expression in isolated NSCs from each group. Sox2; like Nestin, is one of the NSCs markers and is expressed in almost all the NSCs. Values for each groups were normalized to GADPH mRNA levels, then relative expression to SOX2 was calculated (n = 3). 20X Objective, All Scale bars = 100 µm, $P < 0.001$ by Student's unpaired two-tailed t-test. Data shown is mean ± SD.

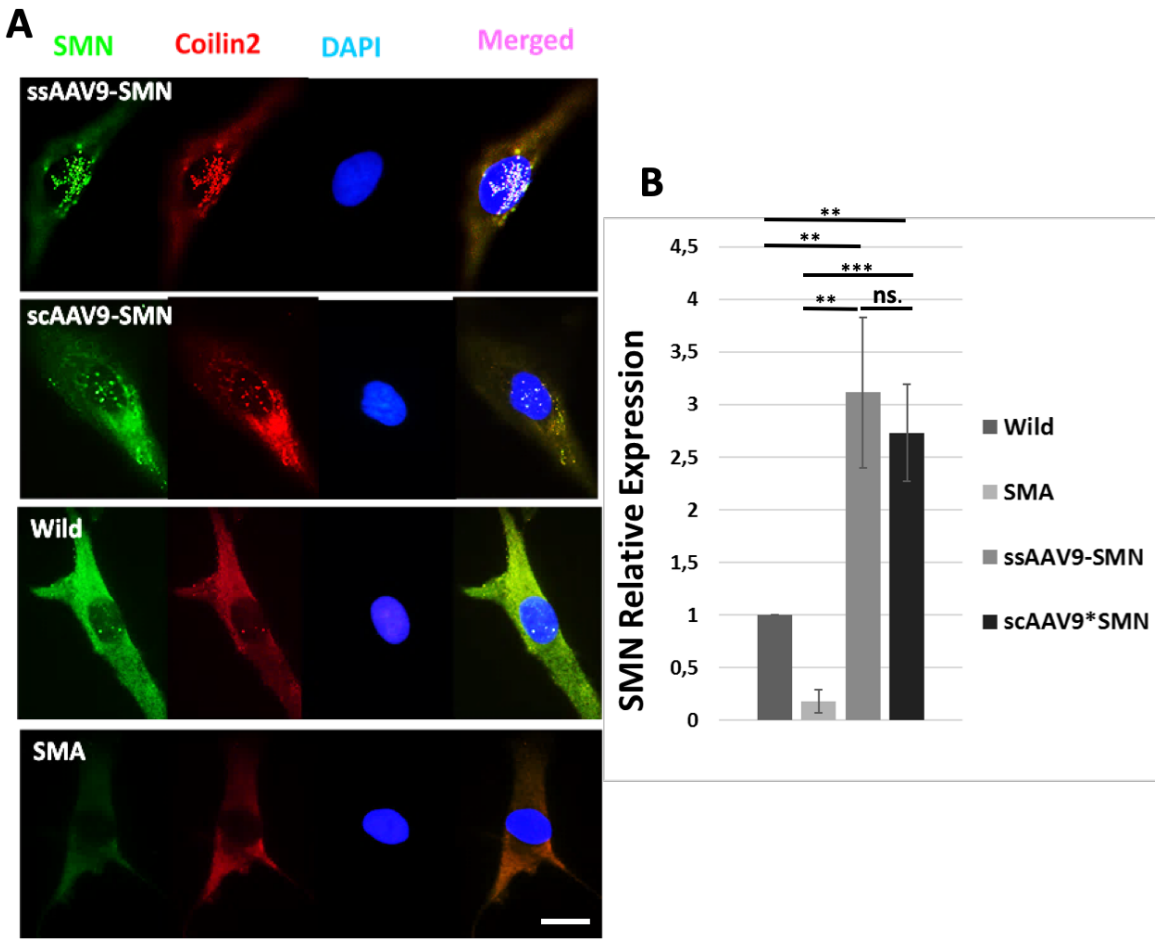


**Figure S7.** rAAV9-SMN restored SMN expression in GEMs. **A**) Co-localization of SMN (green) and Coilin2 (red) in GEM multiproteins in transduced and wild type fibroblasts. The number of the GEMs increased in the both ss and scAAV9-SMN transduced cells compared with wild type or SMA controls. Untreated SMA fibroblast showed a lack of nuclear gems. **B**) qRT-PCR results. ss and scAAV9-SMN vectors led to a significant increase of SMN protein in ss and scAAV9-SMN transduced cells, 3.11±0.71-fold and 2.73±1.46-fold, respectively, compared with wild type controls. There was not a significant difference between these two transduced groups. Data shown is mean ± SD. **P < 0.006, ***P < 0.0007, Scale bar = 100 µm.

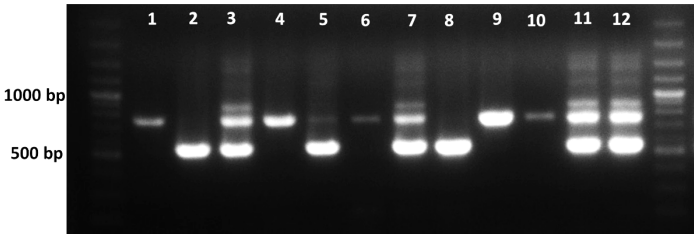


**Figure S8.** Newborn genotyping results. A PCR products with a single 750 bp band demonstrate wild type gene (lane 1, 4, 6, 9, 10), a PCR products with a single 500 bp band demonstrate homozygous mutant (lane 2 and 8), and those with both 700 bp and 500 bp products demonstrate heterozygous genotype (lane 3, 5, 7, 11, and 12). Genotyping was done using 5´-CTC CGG GAT ATT GGG ATT G-3´forward primer, 5´-GGT AAC GCC AGG GTT TTC C-3´ Revers Mutant primer, and 5´-TTT CTT CTG GCT GTG CCT TT-3´ Revers *Wild* type primer. These primers were found in *The Jackson Laboratory* website for genotyping this mouse model (005025).

**Supplemental Tables**

**Table S1.** The number of injected embryos in ICV and IP groups and survival to birth by each group.

| Group | | Embryos injected | Volume (µl) | Vector Genome (vg) | Liveborn pups | % of Survival |
|---|---|---|---|---|---|---|
| IU-ICV | scAAV9-eGFP | 21 | 2 | 4E+10 | 18 | 85.18 |
| | Mock | 6 | – | – | 5 | |
| IU-IP | scAAV9-eGFP | 19 | 5 | 1E+11 | 17 | 92 |
| | Mock | 6 | – | – | 6 | |
| **Total** | – | 52 | – | – | 46 | **88.46** |

**Suplemental Method**

**Isolation and culture of the Mouse NSCs**

The NSCs were isolated by a method described previously[1,2] with some modification to cultivate them as monolayer cells. Briefly, the SVZs from 3-4 week old mice were dissected and pooled. Tissues were minced and incubated for 5-10 min in 1 ml 0.05% trypsin at 37 °C and 0.01% DNase I. The enzyme activity was inhibited by adding equal volume of DMEM-F12 growth media containing 10% FBS, 1% L-glutamine, and 1% Pen-Strep. Pellet was collected by centrifugation at 300 ×g for 5 min. The cells were re-suspended in 4 ml of growth media and pass through 40 µm nylon mesh to remove tissue debris. After centrifugation cells were dissolved in 1 ml growth media supplemented with 2µg/ml Heparin, 20 ng/ml FGF-2 and 20 ng/ml EGF, and cultured in one well of pre-coated 6-wells plate (Celprogen, Torrance, CA, U36110-37-6Well). Cells received fresh growth media containing FGF-2 and EGF, every 3 days. eGFP, Nestin, and Sox2 expressions in NSCs were investigated by immunoflourecence and qRT- PCR analysis.

**Supplemental References**


1- Azari, H., Louis, S.A., Sharififar, S., Vedam-Mai, V., Reynolds, B.A. (2011). Neural-Colony Forming Cell Assay: An Assay To Discriminate Bona Fide Neural Stem Cells from Neural Progenitor Cells, J. Vis. Exp. 49, 2639-3791.

2- Babu, H., Claasen, J.H., Kannan, S., Rünker, A.E., Palmer, T., Kempermann, G. (2011). A protocol for isolation and enriched monolayer cultivation of neural precursor cells from mouse dentate gyrus. Front. Neurosci. 5, 89.